Check for updates

The Journal of Phytopharmacology 2025; 14(4):274-280
Online at: www.phytopharmajournal.com

Research Article

ISSN 2320-480X
JPHYTO 2025; 14(4): 274-280
July- August
Received: 09-05-2025
Accepted: 27-08-2025
Published: 30-09-2025

doi: 10.31254/phyto.2025.14407

Preethy John
Associate Professor, Department of Veterinary Pharmacology and Toxicology, College of Veterinary and Animal Sciences, Mannuthy- 680651, Kerala, India

Nisha A. R.
Professor and Head, Department of Veterinary Pharmacology and Toxicology, College of Veterinary and Animal Sciences, Pookode- 673576, Kerala, India

Suresh N Nair
Associate Professor, Department of Veterinary Pharmacology and Toxicology, College of Veterinary and Animal Sciences, Mannuthy- 680651, Kerala, India

Bibu John Kariyil
Assistant Professor, Department of Veterinary Pharmacology and Toxicology, College of Veterinary and Animal Sciences, Mannuthy- 680651, Kerala, India

Uma Radhakrishnan
Professor and Head, Department of Veterinary Biochemistry and Molecular Biology, College of Veterinary and animal Sciences, Mannuthy- 680651, Kerala, India

Correspondence:
Dr. Preethy John
Associate Professor, Department of Veterinary Pharmacology and Toxicology, College of Veterinary and Animal Sciences, Mannuthy- 680651, Kerala, India
Email: preethy@kvasu.ac.in

Cytotoxic and apoptotic potential of biosynthesised silver nanoparticles in Dalton's lymphoma ascites cells

Preethy John, Nisha A. R., Suresh N Nair, Bibu John Kariyil, Uma Radhakrishnan

ABSTRACT

Background: Nanoparticle-mediated cancer therapies have gained increasing attention due to their targeted action and reduced side effects. Piperlongumine (PPLM), a natural alkaloid, has shown anticancer potential, and its combination with nanotechnology could enhance therapeutic outcomes. Dalton's Lymphoma Ascites (DLA) cells serve as a reliable model for evaluating antineoplastic agents. **Objective:** To evaluate and compare the cytotoxic and apoptotic potential of biosynthesised silver nanoparticles (P-AgNPs), chemically synthesised silver nanoparticles (C-AgNPs), piperlongumine (PPLM), and the standard chemotherapeutic agent 5-fluorouracil (5-FU) against DLA cells, and to elucidate the probable underlying mechanisms of cell death. **Materials and Methods:** The cytotoxicity of test compounds was assessed using the MTT assay, and IC_{50} values were calculated. Trypan blue dye exclusion assay was performed to evaluate cell viability after 3 hours of exposure. Apoptotic changes were observed through Acridine Orange/Ethidium Bromide (AO/EB) dual staining after 24-hour treatment with IC_{50} concentrations. Mechanistic studies included DCF-DA assay for intracellular ROS levels, JC-1 staining for mitochondrial membrane potential, DNA fragmentation assay for DNA damage, and qRT-PCR for gene expression analysis of Caspase-3, p53, and Bcl-2, using GAPDH as reference. **Results:** P-AgNPs showed the highest cytotoxicity with an IC_{50} of 1.25 µg/mL, outperforming PPLM (4.028 µg/mL), 5-FU (326.20 µg/mL), and C-AgNPs (743.60 µg/mL). Trypan blue assay indicated an average reduction in cell viability to 49.07% across all treatments. AO/EB staining revealed late apoptosis in P-AgNP- and PPLM-treated cells, early apoptosis with 5-FU, and minimal apoptotic effect from C-AgNPs. Mechanistic assays showed that P-AgNPs induced a marked increase in ROS and significant mitochondrial membrane depolarisation. DNA fragmentation confirmed apoptosis. Gene expression analysis showed upregulation of Caspase-3 and p53, and downregulation of Bcl-2 in P-AgNP-treated cells. **Conclusion:** Biosynthesised silver nanoparticles (P-AgNPs) demonstrated superior cytotoxic and apoptotic effects in DLA cells compared to chemically synthesised nanoparticles and conventional agents. The enhanced efficacy is attributed to ROS generation, mitochondrial dysfunction, and regulation of apoptotic genes, highlighting P-AgNPs as a promising candidate for anticancer therapy.

Keywords: Silver nanoparticles, Piperlongumine, Cytotoxicity, Apoptosis, DLA cells.

INTRODUCTION

Cancer is currently among one of the leading causes of death worldwide. Current treatments include chemotherapy, radiation and surgery, but all these procedures may damage not only the tumour tissue but also normal tissue. Current problems in the treatment of cancer include low specificity, rapid drug clearance, biodegradation and limited targeting. So new molecules with selective toxicity and potency for cancer treatment have to be investigated.

Nanomedicine, using the treatment with agents of size between 1 and 100 nm is an emerging method for treating cancer. Nanoparticles have many properties such as small size and large surface area that increase the absorption and bioavailability [1]. Green synthesis (biosynthesis) method is gaining great attention in current research and development of nanoparticles. Among the available green methods, utilisation of plant extracts is a rather simple and easy process to produce nanoparticles at large scale relative to bacteria and/or fungi mediated synthesis. The phytochemicals in various plant extracts, especially flavones, amides, alkaloids, terpenoids, carboxylic acids, phenols etc. are capable of reducing metal salts into metal nanoparticles and stabilising them [2].

Piperlongumine, a naturally occurring alkaloid isolated from *Piper longum*, has shown promising anticancer potential in previous studies due to its selective cytotoxicity against cancer cells [3]. However, its therapeutic efficacy can be further enhanced by converting it into nanoparticles.

Dalton's Lymphoma Ascites (DLA) cells were used in this study as a suitable in vitro tumour model. DLA is an established transplantable tumour line that is well-characterised, reproducible, and capable of growing in both solid and ascitic forms [4].

The present study aimed to evaluate the *in vitro* antineoplastic potential of silver nanoparticles (AgNPs) synthesised using piperlongumine (P-AgNPs) and to compare their effects with chemically synthesised silver nanoparticles (C-AgNPs), pure piperlongumine (PPLM), and a standard chemotherapeutic drug, 5-fluorouracil (5-FU) in Dalton's Lymphoma Ascites (DLA) cells.

MATERIALS AND METHODS

Sample preparation

The nanoparticle (biosynthesised) powders were resuspended in distilled water, piperlongumine and 5-FU (M/s Sigma-Aldrich Chemical Co. St. Louis, M O, USA) in PBS, at concentration of two mg/mL, further this stock solution was diluted with RPMI medium to required concentrations [5].

Cytotoxicity studies in DLA cell line

MTT (3- (4, 5- dimethylthiazol- 2- yl)- 2, 5- diphenyltetrazolium bromide assay

The 3- (4, 5- dimethylthiazol- 2- yl)- 2, 5- diphenyltetrazolium bromide (MTT) assay was done [6]. Cell viability was determined by MTT colorimetric assay capable of detecting viable cells by the reduction of the yellow tetrazolium salt to purple formazan. The DLA cells aspirated from the peritoneal cavity of tumour bearing mice were washed thrice with PBS and seeded at a density of $5x10^3$ cells per well in 100 µL medium and were treated with PPLM and P-AgNP (@1.25 µg/mL, 2.5 µg/mL, 5 µg/mL, 10 µg/mL), C-AgNP and 5-FU (@160 µg/mL, 320 µg/mL, 640 µg/mL,1280 µg/mL) for a period of 24 h. After the treatment, 10 µL of MTT (five mg/mL) was added and incubated at 37˚C for four hours. Then the media with MTT was removed and the formed purple formazan crystals were dissolved in 200 µL of DMSO and read at 570 nm in ELISA plate reader (Varioskan Flash, M/s Thermo Fisher Scientific, Finland). The effect of test compounds on cell viability was assessed by comparing the viability of treated cells with that of control cells. Percentage of inhibition was calculated by the formula:

$$\frac{\text{Mean OD of Control- Mean OD of treated cells}}{\text{Mean OD of Control}} \times 100$$

IC_{50} value was obtained from the percentage of inhibition by plotting the concentration against per cent cell inhibition using Graph pad prism. A non-linear regression analysis with a sigmoidal dose–response (variable slope) curve fitting model was employed to interpolate the IC_{50} values.

Trypan blue dye exclusion assay

Trypan blue dye exclusion assay was done as per the modified method of Strober (2001) [7]. The DLA cells aspirated from the peritoneal cavity of tumour bearing mice were washed thrice with PBS. The cells (5×10^5 cells/mL) were added to tubes containing IC_{50} of biosynthesised piperlongumine AgNPs, 5-FU, chemically synthesised AgNPs and volume was made up to one millilitre using PBS. Tubes were incubated for three hours at 37˚C. After incubation, cell viability was assessed by staining one part of cell suspension (10 µL) with one part (10 µL) of trypan blue dye. Using automated cell counter (M/s Invitrogen Life Technologies USA), viable and nonviable cells were counted. All the experiments were carried out in triplicates.

The per cent of viable cells was calculated using the formula:

Acridine orange / Ethidium bromide (AO/EB) staining

A concentration of 5 x 10^5 DLA cells were seeded into a six well cell culture plate and treated with IC_{50} of test compounds and standard drug for 24 h. The acridine orange / ethidium bromide (AO/EB) staining procedure was followed to differentiate the live, apoptotic and necrotic cells. Twenty-five microlitres of the treated or untreated cells were stained with five microlitres of acridine orange (10 µg/mL) and ethidium bromide (10 µg/mL) and analysed under Trinocular Research fluorescence microscope, DM 2000 LED, Leica with blue excitation (488 nm) and emission (550 nm) filters at 20X magnification [8].

Dichlorofluorescein-diacetate (DCF-DA) staining

Intracellular ROS generation was measured by 2', 7' dichlorofluorescein-diacetate (DCF-DA) staining method using the redox sensitive CMH2 DCF-DA fluorescent probe. The DLA cells were seeded along with IC_{50} of test compounds and standard drug into a 96 well cell culture treated plate and incubated for 24 h. After this, cells were incubated with 10 µM DCF-DA at 37˚C for 30 min. The intracellular reactive oxygen species (ROS) mediated oxidation of DCF-DA to the fluorescent compound 2,7- dichlorofluorescein (DCF) was measured using an excitation of 485 nm and emission of 535 nm, in a fluorescence microplate reader [9].

The percentage increase in fluorescence per well was calculated by the formula:

$$\text{Percentage Increase in Fluorescence per well} = \frac{(F_{t30} - F_{t0}) \times 100}{F_{t0}}$$

where Ft_{30} -fluorescence at time 30 min and Ft_0 - fluorescence at time zero.

JC-1 staining

Mitochondrial transmembrane potential (MMP) was analysed by JC-1 staining. The DLA cells were plated at a seeding density of 5×10^4 cells/well in a 12-well plate and treated with test substances and standard drugs at IC_{50}. After 24 h of treatment, cells were incubated with five millimolar JC-1 for 30 min at room temperature in the dark. The cells were analysed directly in the culture medium with filters having excitation/emission of 540/570 nm) and red excitation/emission of 590/610 nm filters using fluorescent microscope (DM 2000 LED, Leica) [10].

DNA fragmentation assay

Deoxyribonucleic acid fragmentation in DLA cells was assayed by the modified method [11]. The DLA cells treated with IC_{50} of test compounds and standard drug for 24 h were collected and washed in PBS. Centrifuged and collected the cell pellet. To the pellet, added one millilitre lytic buffer and vortexed vigorously. Centrifuged at 14,000xg for 10 min at 4˚C. Transferred the supernatant carefully and collected the pellets. Added one millilitre of 25 per cent Trichloroacetic acid (TCA) to tubes containing supernatant and pellet and vortexed vigorously. Allowed precipitation to proceed overnight at 4˚C. After incubation, centrifuged at 14,000xg for 15 min at 4˚C. The obtained supernatant contained fragmented DNA while the intact DNA was present in the pellet. Blank solution used was 25 per cent TCA alone. The amount of DNA in both the supernatant and pellet was estimated using NanoDrop™ 1000 Spectrophotometer.

$$\text{Percent of fragmented DNA} = \frac{\text{Amount of DNA in supernatant}}{\text{Amount of DNA in both the supernatant and pellet}} \times 100$$

Statistical Analysis

The results were analysed using repeated measures ANOVA using SPSS V 24 and post hoc analysis was done by Latin Square Design. Data on cell viability was analysed using student 't' test.

RESULT

Cytotoxicity studies in DLA cell line

MTT (3- (4, 5- dimethylthiazol- 2- yl)- 2, 5- diphenyltetrazolium bromide) assay

The per cent cell viability of DLA cells after 24 h treatment with each of the test compounds and standard drug was determined by MTT reduction assay. The data of MTT reduction assay are presented in Table 1. Dose-response curve of the per cent cell viability plotted with per cent cell viability of DLA cells against various concentrations of test compounds are depicted in Figure 1-3. The percentage of inhibition was calculated and IC_{50} value was obtained from the percentage of inhibition using Graph pad prism (Figure 4-7).

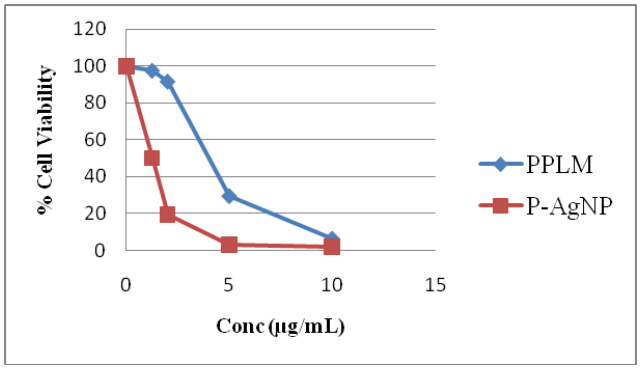

Figure 1: Dose-response curve of the per cent cell viability of DLA cells against various concentrations of PPLM and P-AgNPs

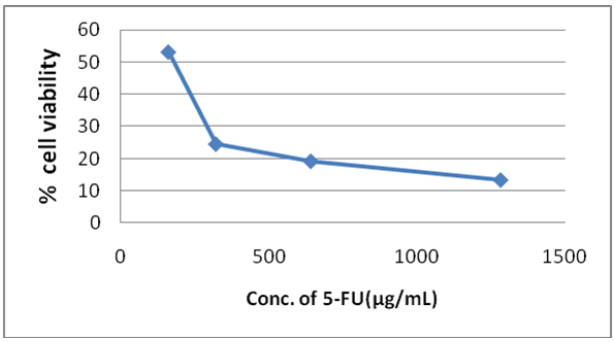

Figure 2: Dose-response curve of the per cent cell viability of DLA cells against various concentrations of 5-FU

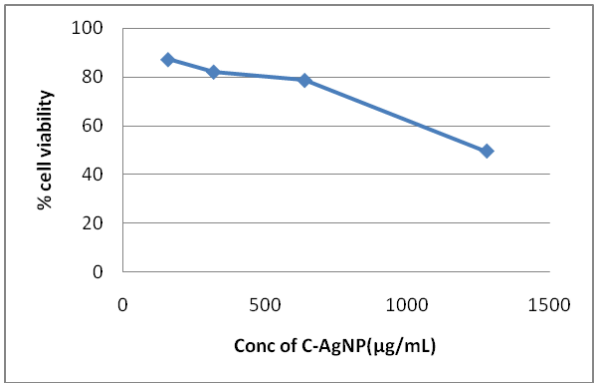

Figure 3: Dose-response curve of the per cent cell viability of DLA cells against various concentrations of C-AgNPs

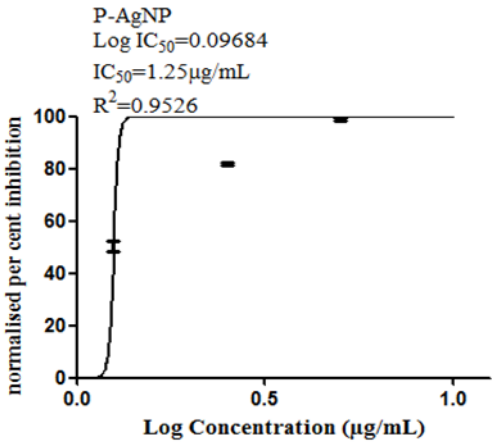

Figure 4: IC_{50} of P-AgNPs

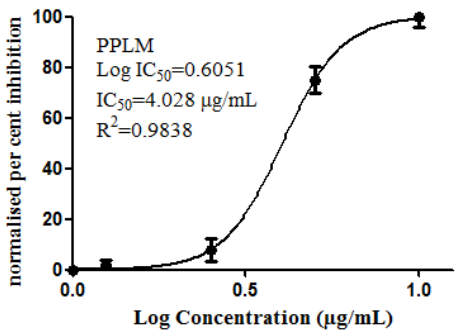

Figure 5: IC_{50} of PPLM

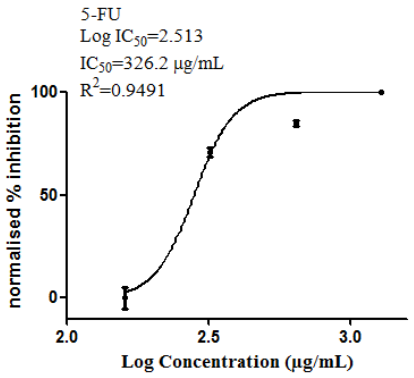

Figure 6: IC_{50} of 5-FU

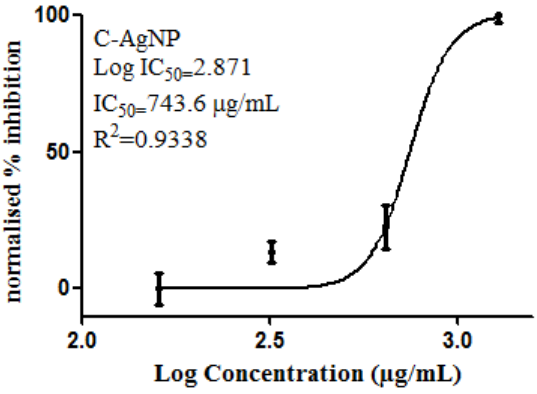

Figure 7: IC_{50} of C-AgNPs

All treatments exhibited concentration dependent cytotoxicity after 24 h of treatment with least viability at high concentration. Per cent cell inhibition of DLA cells after 24 h treatment with various concentrations of test compounds is depicted in Table 1. The half maximal inhibitory concentration (IC_{50}) of P-AgNP was calculated as 1.25 µg/mL Figure 4. Piperlongumine inhibited 50 per cent cells (IC_{50}) at 4.028 µg/mL (Figure 5). The standard drug, 5-FU and C-AgNPs imparted minimal cytotoxicity after 24 h treatment, with IC_{50} values calculated as 326.2 (Figure 6) and 743.6 µg/mL (Figure 7) respectively.

Table 1: Per cent cell inhibition of DLA cells after 24 h treatment with various concentrations of test compounds determined by MTT

Conc. µg/mL	Cell inhibition (%)		Conc. µg/mL	Cell inhibition (%)	
	PPLM	P-AgNP		5-FU	C-AgNP
1.25	2.50 ±2.03	49.73 ± 2.01	160	48.43 ± 2.08	12.77 ± 2.14
2.5	8.43 ± 4.20	80.45 ± 0.51	320	75.50 ± 0.93	17.90 ± 1.40
5	70.42 ± 5.04	96.77 ± 0.49	640	80.86 ± 0.62	21.35 ± 2.97
10	93.48 ± 3.75	97.95 ± 0.11	1280	86.72 ± 0.11	50.58 ± 1.16

Values expressed as mean ±SEM (n=3)

Trypan blue dye exclusion assay

Trypan blue exclusion assay showed that all test compounds reduced cell viability to an average of 49.07% within three hours (Table 2), highlighting their potential to induce cell death in DLA cells.

Table 1: No of viable cells and per cent cell viability on DLA cells after three hours treatment with IC_{50} of test compounds determined by trypan blue dye exclusion assay

Test compounds	No of viable cells after 3 h ($x10^5$)	Cell viability (%)
Control	4.80 ± 0.05^{a}	95.93 ± 1.07^{a}
PPLM	2.32 ± 0.04^{de}	46.45 ± 0.72^{de}
P- AgNP	2.24 ± 0.02^{e}	44.82 ± 0.43^{e}
5-FU	2.52 ± 0.04^{c}	50.33 ± 0.78^{c}
C- AgNP	2.71 ± 0.04^{b}	54.23 ± 0.78^{b}
F-value (P-value)	492.80** (<0.001)	492.80** (<0.001)

Values expressed as mean ± SEM, n=3, Means bearing similar superscript within each column do not differ significantly at p<0.05
PPLM (Piperlongumine), P- AgNP (Piperlongumine Nanoparticle), 5-FU (5-Fluorouracil), C-AgNP (Chemically synthesised Nanoparticle)

Microscopic studies using Acridine orange / Ethidium bromide (AO/EB) staining

The AO/EB dual staining was done to detect the live, early apoptotic, late apoptotic and necrotic cells after treatment with IC_{50} concentration of test compounds and synthesised AgNPs. The representative images of cells of various treatments are given in figure 8 (A-G).

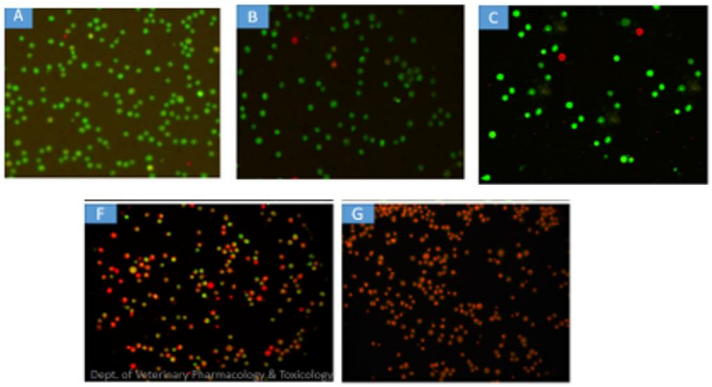

Figure 8: AO/EB staining of DLA cells (20X magnification); A- control cells; B, C, F, G- cells treated with IC_{50} of C-AgNPs, 5-FU, PPLM, P-AgNPs respectively

In control (A), all the cells were live showing greenish fluorescence with circular nucleus uniformly distributed in the centre of the cell. Majority of the cells treated with C-AgNPs (B) were live showing green fluorescence and only few cells were there with orange nucleus. Cells exposed to 5-FU (C). On exposure to PPLM (F) and P-AgNPs (G), numerous cells were in late apoptotic stage with condensed and asymmetrically localised orange-stained nucleus.

Intracellular Reactive Oxygen Species (ROS) generation assay

As shown in the Table 3, an increasing trend in fluorescent intensities of 165.38 per cent, 177.75 per cent, 240.68 per cent, 352.07 per cent were observed in the order C-AgNPs, 5-FU, PPLM and P-AgNPs respectively, as compared with untreated control (100 per cent). Fluorescent intensity corresponds to levels of ROS generated. Thus, a significant (p>0.05) induction in ROS generation was measured in DLA cells exposed to P- AgNPs and PPLM.

Table 3: Effect of treatments on intracellular ROS generation after 24 h treatment with IC50 of test compounds determined by DCF DA assay

Test compounds	Relative fluorescence intensity
Control	100
5-FU	177.75 ± 4.45^{c}
PPLM	240.68 ± 1.48^{b}
P-AgNP	352.07 ± 6.41^{a}
C-AgNP	165.38 ± 4.63^{d}
F-value (P-value)	484.08** (<0.001)

Values expressed as mean ± SEM, n=3, Means bearing similar superscript within each column do not differ significantly at p<0.05
PPLM (Piperlongumine), P- AgNP (Piperlongumine Nanoparticle), 5-FU (5-Fluorouracil), C-AgNP (Chemically synthesised Nanoparticle)

DNA fragmentation assay

The result of DNA fragmentation assay is depicted in Table 4. The amount of intact and fragmented DNA estimated using NanoDrop™ 1000 Spectrophotometer revealed a significant (p<0.05) increase of DNA fragmentation in treated cells compared to untreated cancer control cells. Among the treatments, 5-FU and P-AgNPs treated cells showed an extensive DNA fragmentation than PPLM. The C-AgNPs exposed cells exhibited least per cent of DNA fragmentation.

Table 4: Effect of treatments on DNA fragmentation in DLA cells after 24 h treatment with IC 50 of test compounds, %

Test compounds	DNA fragmentation (%)
Control	10.71 ± 0.61[f]
C-AgNP	42.64 ± 0.71[e]
PPLM	88.12 ± 0.70[b]
P-AgNP	95.40 ± 0.45[a]
5-FU	96.88 ± 0.63[a]
F-value (P-value)	2705.13** (<0.001)

Values expressed as mean ± SEM, n=3, Means bearing similar superscript within each column do not differ significantly at p<0.05
PPLM (Piperlongumine), P- AgNP (Piperlongumine Nanoparticle), 5-FU (5-Fluorouracil), C-AgNP (Chemically synthesised Nanoparticle)

Analysis of mitochondrial transmembrane potential (MMP)

The technique of 5,5,6,6'-tetrachloro-1,1',3,3'tetraethylbenzimidazoylcarbocyanine iodide (JC-1) staining illustrates the change in the mitochondrial membrane potential level. Figure 9 (A-E) depicts the change in the MMP level. A remarkable change in the fluorescence from red to green was observed when DLA cells were exposed to IC_{50} of test compounds. In untreated tumour control cells, JC-1 dye accumulated in the mitochondria as aggregates and was visualised as red fluorescent cells under fluorescent microscope. In cells exposed to treatment, as the MMP declined, the dye was dispersed throughout the cell as monomers and was observed as green fluorescent cells.

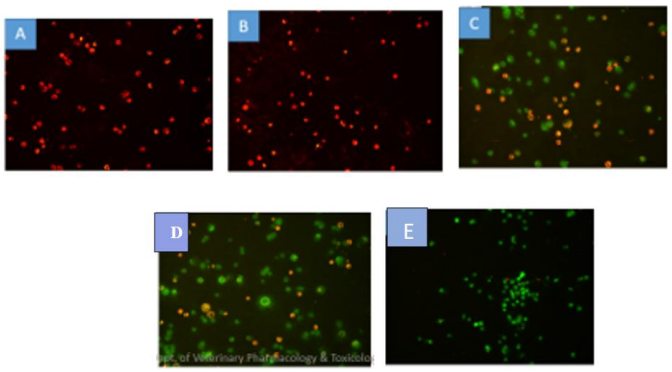

Figure 9: JC 1 staining of DLA cells (20X magnification); A- control cells; B, C, D, E- cells treated with IC50 of C-AgNPs, 5-FU, PPLM, P-AgNPs respectively

DISCUSSION

In the present study cytotoxicity of test compounds and nanoparticles on DLA cells was determined by MTT reduction assay. The MTT could be converted into a purple formazan product with an absorbance near 570 nm by live cells with active metabolism only [12]. So, the purple colour formation served as a useful and convenient marker of the viable cells.

In the present study, after 24 h treatment, the IC_{50} value for PPLM was 4.028 µg/ mL while the value reduced to 1.25 µg/ mL for AgNPs synthesised from PPLM (P- AgNPs). In both HepG2 and MCF-7 cells, the IC_{50} of paclitaxel and PPLM coloaded nanoparticles were lower than that of free paclitaxel and free PPLM [13]. From this it could be assumed that nanonisation could improve the solubility and thus bioavailability [14]. It can also alter the pharmacokinetics and improve drug efficacy.

The trypan dye exclusion test was employed in the current study to determine the number of viable cells present in the cell suspensions incubated with test compounds. This method which is based on the principle that viable cells exclude trypan blue, whereas dead cells stain blue due to trypan blue uptake gives an accurate number of viable and dead cells [15].

All test compounds in the current study showed an average of 49.07 per cent cell viability in three hours. After three hours of exposure to IC_{50} of zinc oxide nanoparticles prepared from hydroethanol *Turbinaria conoides* extract, 55 per cent cell viability in DLA cells was observed [16].

Biosynthesised P-AgNPs and PPLM treated cells showed morphological changes like orange fluorescence and condensed nuclei. These results by AO/EB double staining confirmed that P-AgNPs and PPLM could induce cell death through late apoptosis. However, early apoptotic changes were noticed in 5-FU treated cells. In contrast, the untreated tumour control cells and C-AgNP treated cells were live showing intact nuclear architecture with light green fluorescence.

Morphological features of apoptosis such as nuclear fragmentation, chromatin condensation, alterations in the shape and size of cells, as revealed by fluorescence microscopic analysis were observed after treatment with *Anthocephalus cadamba* on DLA cells [17]. They observed that healthy cells had green nuclei and uniform chromatin with intact cell membrane while the cells undergoing apoptosis had orange nuclei with condensed chromatin and the necrotic cells had red nuclei with damaged cell membrane.

The live cell nucleus presented a green fluorescence, while the apoptotic cell nucleus (PPLM treated human osteosarcoma cells) showed an orange fluorescence and the structure became condensed [18].

To investigate the potential role of biosynthesised AgNPs to induce oxidative stress in DLA cells, intracellular ROS generation was assessed by DCF-DA dye. The DCF-DA, a nonfluorescent dye which diffuses through cell membranes get hydrolysed by intracellular esterases to DCFH. In the presence of ROS, DCFH is oxidised to fluorescent DCF and its level is proportional to the level of generated ROS [19].

The AgNPs induced ROS formation that could mediate oxidative stress and cell death in mouse lymphoma cells [20]. In a previous study, it was demonstrated that plant-synthesised (*Nepeta deflersiana)* AgNPs had the capacity to induce ROS generation, lipid peroxidation along with a decrease in mitochondrial membrane potential (MMP) and glutathione (GSH) levels [21].

The intensity of DCFH-DA fluorescence (representing the ROS level) in the primary bone marrow mononuclear cells was significantly($p>0.05$) increased at 24 h of PPLM treatment, in a dose-dependent manner [22].

An increase in the fluorescence intensity in biosynthesised AgNPs treated cells observed in the present study established that biosynthesised AgNPs induced more ROS generation, which led to oxidative stress and cancer cell death.

In the present study, exposure of DLA cells to IC_{50} of test compounds revealed a significant ($p>0.05$) increase in per cent of DNA fragmentation. The DNA fragmentation is considered as a characteristic feature of apoptosis [23]. The ROS can act as signal molecules that can induce oxidative DNA damage. The DLA control cells exhibited negligible fragmentation whereas a minimum fragmentation was noticed in C-AgNPs treated cells. The groups treated with 5-FU and P-AgNPs exhibited extensive fragmentation followed by PPLM. This implied that biosynthesised AgNPs possess apoptotic inducing effect by causing DNA damage.

The AgNPs could induce apoptosis by DNA fragmentation [24] and PPLM -induced ROS is responsible for DNA damage in pancreas cancer cells [25].

The JC-1 (5,5,6,6-tetrachloro-1,1,3,3-tetraethylbenzimidazolyl-carbocyanine iodide) staining was carried out in DLA cells treated with IC_{50} of test compounds to investigate whether these compounds induced apoptosis *via* disruption of MMP. In the control, JC-1 exhibited a red fluorescence and after DLA cells were exposed to test compounds for 24 h, JC-1 showed a gradual increase in green fluorescence (with little red fluorescence) which implies decrease in MMP. A change from red to green fluorescence indicated a decrease in MMP following cisplatin treatment [26].

In the present study, a few cells with red fluorescence and a few with green fluorescence was found in the cells treated with 5-FU. But on PPLM and P-AgNPs treatment more green fluorescent cells were visualised. These findings are consistent with those of earlier research.

co-treatment of apigenin with 5-FU lowered mitochondrial membrane potential and consequently promoted mitochondrial apoptosis in hepatocellular cancer [27]. A dose-dependent reduction in mitochondrial membrane potential was observed when melanoma cells were exposed to increasing concentrations of PPLM [28].

The JC-1, a lipophilic, cationic dye (naturally exhibiting green fluorescence) was able to enter into the cells with a normal MMP where it accumulates in the negatively charged mitochondria and spontaneously forms red fluorescent J-aggregates [29]. Therefore, in the present study, in cancer control cells, the negative charge established in the intact mitochondrial membrane potential might have allowed this cationic dye to enter the mitochondrial matrix where it accumulated as J-aggregates that were visualised as red fluorescent cells using fluorescent microscope.

When there is an alteration in the permeability of the inner mitochondrial membrane, mitochondrial permeability transition (MPT) occurs [30]. So, in cells that undergone treatment, increased membrane permeability made mitochondrial matrix less negative which allow the entry of JC 1 stain only to a less degree. Since JC-1 could not reach a sufficient concentration to trigger the formation of J-aggregates, thus retaining its original green fluorescence in the apoptotic cells. These results suggested that the biosynthesised AgNPs and PPLM could reduce the membrane potential and induce mitochondrial dysfunction. Increase in ROS levels induced by AgNPs was accompanied by a reduction of MMP [31].

The MPT released apoptogenic components into the cytosol, activating a caspase proteolytic cascade accelerated by a positive feedback loop involving the release of mitochondrial cytochrome c (Cyt-c) and ultimately inducing apoptosis [32]. Therefore, the results of present study demonstrated that test compounds induced a decrease in mitochondrial membrane potential and induced apoptosis in the DLA cells through a mitochondrial signal transduction pathway.

CONCLUSION

In our study, biosynthesised silver nanoparticles (P-AgNPs) exhibited superior cytotoxic and pro-apoptotic effects in Dalton's lymphoma ascites (DLA) cells compared to chemically synthesised nanoparticles and conventional chemotherapeutic agents. The enhanced efficacy of P-AgNPs appears to be mediated through a mechanistic cascade involving elevated ROS generation, disruption of mitochondrial membrane potential, and modulation of apoptosis-related gene expression, particularly the downregulation of *Bcl-2*. This ROS-driven, mitochondria-dependent pathway underscores the potential of P-AgNPs as a promising candidate for anticancer therapy. Further in-depth mechanistic and in vivo studies are warranted to validate their therapeutic applicability and safety.

Acknowledgments

The acknowledgments of the funding body, institutional head, co-workers, field assistants, local people etc. should be briefed and declaration of any conflict of interest related to the work.

Conflict of interest

The authors declared no conflict of interest.

Financial Support

None declared.

ORCID ID

Preethy John: https://orcid.org/0000-0002-7973-8205

REFERENCES

1. Shi J, Kantoff P, Wooster R, Farokhzad OC. Cancer nanomedicine: progress, challenges and opportunities. Nat Rev Cancer. 2017;17:20–37.
2. Aromal SA, Philip D. Green synthesis of gold nanoparticles using *Trigonella foenum-graecum* and its size-dependent catalytic activity. Spectrochim Acta A Mol Biomol Spectrosc. 2012;97:1–5.
3. Duan C, Zhang B, Deng C, Cao Y, Zhou F, Wu L, *et al*. Piperlongumine induces gastric cancer cell apoptosis and G2/M cell cycle arrest both *in vitro* and *in vivo*. Tumour Biol. 2016;37:10793–804.
4. Koiri RK, Mehrotra A, Trigun SK. Dalton's lymphoma as a murine model for understanding the progression and development of T-cell lymphoma and its role in drug discovery. Int J Immunother Cancer Res. 2017;3:1–6.
5. Bimitha B, Krishna AS, Sujith S, Preethy J, Uma R. Cytotoxic and antiproliferative potential of methanolic extract of *Mallotus phillippensis* in MCF-7 cell line. J Phytopharmacol. 2022;11:60–3.
6. Naidu VG, Mahesh BU, Giddam AK, Babu KR, Ding J, Babu KS, et al. Apoptogenic activity of ethyl acetate extract of leaves of *Memecylon edule* on human gastric carcinoma cells via mitochondrial dependent pathway. Asian Pac J Trop Med. 2013;6:337–45.
7. Strober W. Trypan blue exclusion test of cell viability. Curr Protoc Immunol. 2001;3:3.
8. Ribble D, Goldstein NB, Norris DA, Shellman YG. A simple technique for quantifying apoptosis in 96-well plates. BMC Biotechnol. 2005;5:1–7.
9. Kim HJ, Suh HJ, Kim JH, Park S, Joo YC, Kim JS. Antioxidant activity of glyceollins derived from soybean elicited with *Aspergillus sojae*. J Agric Food Chem. 2010;58:11633–8.
10. Ovadje P, Chatterjee S, Griffin C, Tran C, Hamm C, Pandey S. Selective induction of apoptosis through activation of caspase-8 in human leukemia cells (Jurkat) by dandelion root extract. J Ethnopharmacol. 2011;133:86–91.
11. Kurita-Ochiai T, Fukushima K, Ochiai K. Lipopolysaccharide stimulates butyric acid-induced apoptosis in human peripheral blood mononuclear cells. Infect Immun. 1999;67:22–9.
12. Riss TL, Moravec RA, Niles AL. Cell viability assays. In: Markossian S, Sittampalam GS, Grossman A, et al., editors. Assay Guidance Manual [Internet]. Bethesda (MD): Eli Lilly & Company and the National Center for Advancing Translational Sciences; 2013 May 1 [updated 2016 Jul 1].
13. Liu Q, Zhao D, Zhu X, Chen H, Yang Y, Xu J, *et al*. Coloaded nanoparticles of paclitaxel and piperlongumine for enhancing synergistic antitumor activities and reducing toxicity. J Pharm Sci. 2017;106:3066–75.

14. Prakash S, Sasidhar R, Abhijit D. Nanonisation: a novel approach for enhancement of bioavailability of poorly soluble drugs. J Nanopharm Drug Deliv. 2013;1:227–39.
15. Kuttan R, Bhanumathy P, Nirmala K, George MC. Potential anticancer activity of turmeric (*Curcuma longa*). Cancer Lett. 1985;29:197–202.
16. Raajshree RK, Durairaj B. In vitro anticancer potential of biosynthesised zinc oxide nanoparticles from the seaweed *Turbinaria conoides*. Asian J Pharm Clin Res. 2018;11:127–30.
17. Dolai N, Islam A, Haldar PK. Antiproliferative activity and apoptosis inducing mechanism of *Anthocephalus cadamba* on Dalton's lymphoma ascites cells. Iran J Pharm Res. 2016;15(3):505–514.
18. Zhou J, Huang Z, Ni X, Lv C. Piperlongumine induces apoptosis and G2/M phase arrest in human osteosarcoma cells by regulating ROS/PI3K/Akt pathway. Toxicol In Vitro. 2020;65:104775.
19. Eruslanov E, Kusmartsev S. Identification of ROS using oxidised DCFDA and flow-cytometry. Methods Mol Biol. 2010;594:57–72.
20. Mei N, Zhang Y, Chen Y, Guo X, Ding W, Ali SF, *et al*. Silver nanoparticle-induced mutations and oxidative stress in mouse lymphoma cells. Environ Mol Mutagen. 2012;53(6):409–419.
21. Al-Sheddi ES, Farshori NN, Al-Oqail MM, Al-Massarani SM, Saquib Q, Wahab R, et al. Anticancer potential of green synthesised silver nanoparticles using extract of *Nepeta deflersiana* against human cervical cancer cells (HeLa). Bioinorg Chem Appl. 2018;2018:1–12.
22. Xiong XX, Liu J, Qiu X, Pan F, Yu SS, Chen X. Piperlongumine induces apoptotic and autophagic death of the primary myeloid leukemia cells from patients via activation of ROS-p38/JNK pathways. Acta Pharmacol Sin. 2015;36(3):1–13.
23. Allen RT, Hunter WJ, Agrawal DK. Morphological and biochemical characterisation and analysis of apoptosis. J Pharmacol Toxicol Methods. 1997;37(4):215–228.
24. Sriram MI, Kanth SB, Kalishwaralal K, Gurunathan S. Antitumor activity of silver nanoparticles in Dalton's lymphoma ascites tumor model. Int J Nanomed. 2010;5:753–762.
25. Dhillon H, Chikara S, Reindl KM. Piperlongumine induces pancreatic cancer cell death by enhancing reactive oxygen species and DNA damage. Toxicol Rep. 2014;1:309–318.
26. Choi YM, Kim HK, Shim W, Anwar MA, Kwon JW, Kwon HK, *et al*. Mechanism of cisplatin-induced cytotoxicity is correlated to impaired metabolism due to mitochondrial ROS generation. PLoS One. 2015;10(8):e0135083.
27. Hu XY, Liang JY, Guo XJ, Liu L, Guo YB. 5-Fluorouracil combined with apigenin enhances anticancer activity through mitochondrial membrane potential (ΔΨm)-mediated apoptosis in hepatocellular carcinoma. Clin Exp Pharmacol Physiol. 2015;42(2):146–153.
28. Song X, Gao T, Lei Q, Zhang L, Yao Y, Xiong J. Piperlongumine induces apoptosis in human melanoma cells via reactive oxygen species mediated mitochondria disruption. Nutr Cancer. 2018;70(3):502–511.
29. Sivandzade F, Bhalerao A, Cucullo L. Analysis of the mitochondrial membrane potential using the cationic JC-1 dye as a sensitive fluorescent probe. Bio Protoc. 2019;9(1):e3128.
30. Hunter DR, Haworth RA. The Ca2+-induced membrane transition in mitochondria. I. The protective mechanisms. Arch Biochem Biophys. 1979;195:453–459.
31. Onodera A, Nishumi F, Tanaka A, Tanabe N, Honma A, Yayama K, *et al*. Short-term changes in intracellular ROS localisation after silver nanoparticles exposure depending on particle size. Toxicol Rep. 2015;2:574–579.
32. Wang C, Youle RJ. The role of mitochondria in apoptosis. Annu Rev Genet. 2009;43:95–118.

HOW TO CITE THIS ARTICLE

John P, Nisha AR, Nair SN, Kariyil BJ, Radhakrishnan U. Cytotoxic and apoptotic potential of biosynthesised silver nanoparticles in Dalton's lymphoma ascites cells. J Phytopharmacol 2025; 14(4):274-280. doi: 10.31254/phyto.2025.14407